Concepts for the Liquefaction of Hydrogen for In-Situ Operations on the Lunar or Martian Surface

Wesley L Johnson[1]
NASA Glenn Research Center, Cleveland, OH 44135, USA

While oxygen will probably be the first fluid liquefied from in-situ developed propellants, hydrogen will also be a sought-after commodity on both the Lunar and Martian surfaces. General hydrogen liquefaction processes are not significantly affected by the atmosphere on Mars and similar processes can be applied on both surfaces. However, hydrogen will require different processes than oxygen (which can be directly liquefied into its final use tank) due to the different spin states the hydrogen nucleus (i.e. parahydrogen and orthohydrogen) can have as well as the significant sensible energy that has to be removed prior to the actual phase change. Due to the low efficiency of 20 K class flight-rated cryocoolers and high sensible heat removal requirements at higher temperatures, significant benefits can be obtained by precooling the hydrogen gas in a variety of manners. The benefits of three concepts are explored to take advantage of different precooling techniques as well as accounting for sensible, latent, and para to ortho conversion heating requirements. Process concepts are shown that can reduce the base input power requirements for heat removal by more than 67% and the radiator area by similar amounts. A majority of the technology development for these processes has already begun, both within NASA and externally, with the few gaps being identified.

I. Nomenclature (to be updated once equations all filled in)

A	=	a constant used to define the efficiency of a cryocooler relative to the Carnot efficiency
h	=	specific enthalpy of the state defined in the parenthesis that follow it, J/g
$h_{convert}$	=	enthalpy of conversion from orthohydrogen to parahydrogen, J/g
$\dot{m}$	=	mass flow rate, g/s
P	=	pressure, kPa
$\dot{Q}$	=	heat flow, W
T	=	temperature, K
Greek		
γ	=	mass fraction of a type of hydrogen
η	=	efficiency of a system
Subscripts		
c	=	cold or temperature at which heat is removed in a refrigeration cycle
Carnot	=	the efficiencies as defined as an ideal system
h	=	hot or temperature at which heat is rejected in a refrigeration cycle
h2	=	hydrogen (both para and ortho types combined)
i	=	incoming flow
liq	=	liquid properties
liquefaction	=	the energy required to be removed for phase change from gas to liquid
o	=	outgoing flow

[1] Cryogenics Team Lead, Fluid and Cryogenic Systems Branch, AIAA Senior Member.

otop = ortho to para
para = of the parahydrogen type
remove = the total energy required to be removed by a cooling mechanism
sat = saturation properties of a two phase system
sensible = the change in sensible heat (i.e. the energy required to change the temperature of a gas flow)

II. Introduction

One of the more intriguing places on the lunar surface, both due to the cryogenic applications and the resources that are present, are the permanently shadowed regions (PSRs) of the moon. These are regions, generally in craters, at the north and south poles that don't directly receive any energy from the sun. Similarly, around these craters are areas that receive sun over 90% of the time[1]. The areas that don't receive sunlight have been measured at temperatures as cold as 35 K[2], providing a cold trap for ice as well as a cryogenic environment. Over the last 10 years, since the Lunar Reconnaissance Orbiter and Lunar Crater Observation and Sensing Satellite (LCROSS) provided some of the first insight into these areas, there has been quite a bit of analysis and speculation on the engineering that could be accomplished in these environments.

Many scientists and engineers are excited about exploring these areas. Metzger[3] has laid out a whole development plan that centers on first developing the capability of extracting water ice from these stores and then processing this into hydrogen and oxygen to eventually refuel vehicles from an orbital propellant depot. Similarly, the United Launch Alliance (ULA) held a workshop to discuss methodologies to process the water ice all the way to usable commodity[4]. Furthermore, NASA has begun to fund the development of these resources in order to feed into the sustainable lunar architecture concepts[5]. To provide more detailed information on the actual resources within these PSRs, NASA recently announced the Volatiles Investigating Polar Exploration Rover (VIPER)[6].

Unfortunately, the thermodynamics of the liquefaction process has not been accounted for in many of the studies to date. Many point to the low temperatures of the surfaces within the PSRs and claim that liquefaction of at least the oxygen if not the hydrogen will be "free" (i.e. require little to no resources). This assumption does not consider that the gas coming out of the electrolyzers that are nearly universally employed to separate water into the constituent hydrogen and oxygen, imposes a heat load into the environment. While burying a heat exchanger in the polar pits may at some point be possible as robots and civil engineering capability is developed with the constitution of the bottom of the craters understood, this capability will not be readily available in the initial waves of development. With the lack of an atmosphere on the moon, the remaining passive heat rejection method is radiation. Radiation is an excellent transmitter of energy at relatively high temperatures, however, as the temperature decreases, the energy emitted decreases by that temperature to the fourth power (T^4). At 300 K, a radiator to deep space with an emissivity of 0.8 can emit over 360 W/m^2 that same radiator at 90 K can only emit 3 W/m^2.

III. Configurations Evaluated

While oxygen liquefaction without any precooling below 300 K and direct insertion into the storage tank has recently been demonstrated[7], that demonstration does not fully cover the liquefaction of hydrogen. There are two main differences between hydrogen and oxygen or methane liquefaction. The sensible heat of hydrogen between 300 K and the normal boiling point is approximately 6 times that of the latent heat (for oxygen and methane, the sensible heat is less than the latent heat). Hydrogen molecules occur in two spin/energy states: parahydrogen and orthohydrogen. Temperature influences hydrogen's magnetic state and the conversion from ortho to parahydrogen is exothermic[8]. The former in combination with the relative inefficiency of 20 K class flight-rated cryocoolers requires that the precooling of hydrogen be considered in much more detail than that of oxygen and methane. The latter requires incorporation of para-to-ortho conversion reactors to be incorporated into the design of the precooling systems as the para-to-ortho conversion is an exothermic reaction and that generated heat must be removed.

Four different configurations for hydrogen liquefaction were evaluated: all heat removed at 20 K via cryocooler, precooling via radiator (see Figure 1), precooling via cryocooler at an intermediate temperature (between 300 K and 20 K, see Figure 2), and with both precooling options in use (see Figure 3). For the latter three concepts, any heat not removed by the precooling stages is removed by a 20 K cryocooler, including accounting for the final para to ortho conversion. All cryocoolers, both 20 K and 90 K assumed a heat rejection temperature of 300 K. Optimization of the heat rejection temperature between mass of the radiator, mass of power production, and cryocooler mass is a separate trade.

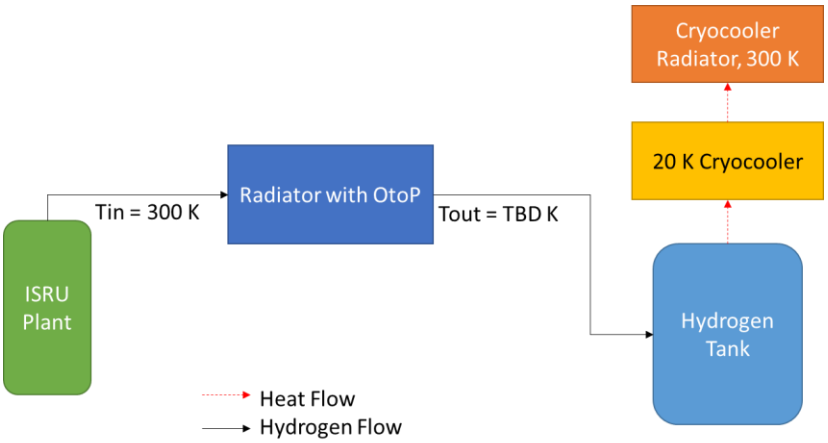

Figure 1: Radiator Only Precooling Configuration

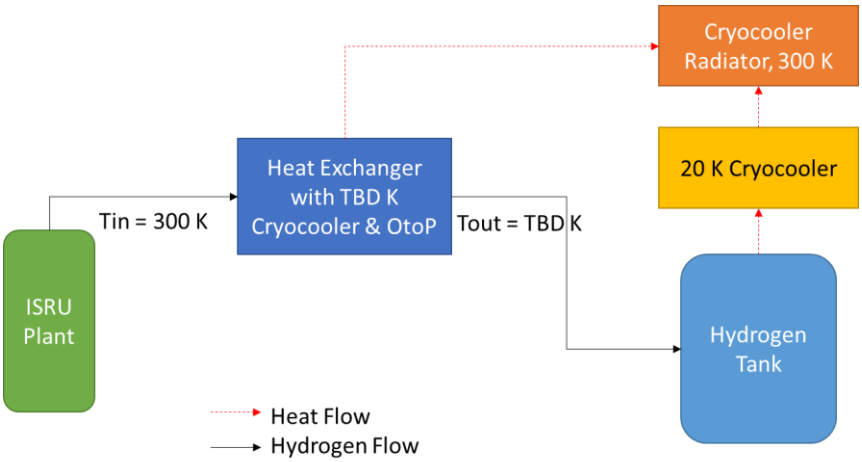

Figure 2: Intermediate Cryocooler Only Precooling Configuration

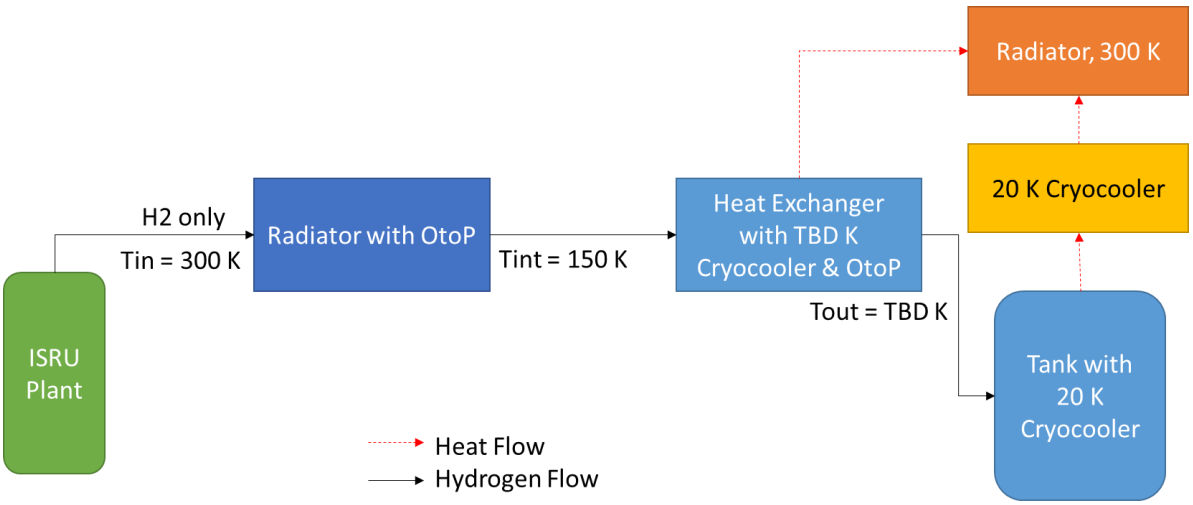

Figure 3: Radiator and Intermediate Cryocooler Precooling Configuration

IV.Mathematical Model

A simple model was assembled based on known development on 90 K class (range between 120 K and 70 K) and 20 K class cryocoolers[9] and the process that the hydrogen goes through as it is first pre-cooled and then liquefied.

A. Hydrogen Fluid Model

The hydrogen thermal state was modeled using constant pressure, temperature dependent properties of parahydrogen and orthohydrogen properties from NIST's REFPROP[10]. The amount of parahydrogen and orthohydrogen was determined by temperature dependent equilibrium properties published by Flynn[11]. The transition between parahydrogen and orthohydrogen was determined by the change in the equilibrium percentages as well as the heat of conversion at the appropriate temperature as shown in Eq. 1. The conversion of hydrogen from ortho to para states is assumed to be 100% effective and that the gas that exist the heat exchanger is the same ratio para to ortho fractions as the equilibrium. The energy that has to be removed to change the temperature of the hydrogen flow is shown in Eq. 2. The sum of the energy removed must be the sum of the two energy types as shown in Eq 3. These hold for all steps except the final step where the actual phase change occurs in which case Eq 4 replaces Eq 2 and Eq 5 replaces Eq 3. Since the assumption is made at all states that the ortho to para hydrogen conversion is 100% effective at that temperature, normal hydrogen properties can be used as a substitute for the para and ortho specific enthalpies. However, if at some point the conversion is assumed to be less than 100% effective, the equations must be used as stated in Eq 2 and Eq 4.

$$\dot{Q}_{otop} = \dot{m}_{h2} h_{convert}(T_{otop})(\gamma_{para,o} - \gamma_{para,i}), \tag{1}$$

$$\dot{Q}_{sensible} = \dot{m}_{h2}\left(h_{para}(T_o)\gamma_{para,i} + h_{ortho}(T_o)\gamma_{ortho,i} - h_{para}(T_i)\gamma_{para,i} - h_{ortho}(T_i)\gamma_{ortho,i}\right), \tag{2}$$

$$\dot{Q}_{remove} = \dot{Q}_{sensible} + \dot{Q}_{otop}, \tag{3}$$

$$\dot{Q}_{liquefaction} = \dot{m}_{h2}\left(h_{para,liq}(P_{sat})\gamma_{para,i} + h_{ortho}(T_o)\gamma_{ortho,i} - h_{para}(T_i)\gamma_{para,i} - h_{ortho}(T_i)\gamma_{ortho,i}\right), \tag{4}$$

$$\dot{Q}_{remove,liquefaction} = \dot{Q}_{sensible} + \dot{Q}_{otop}, \tag{5}$$

B. Radiator

The radiator was modeled as a variable temperature radiator in that enthalpy of the hydrogen flow was updated every 5 K and the radiator area was calculated for that 5 K segment based on the lower temperature of the 5 K range. Equations 1 and 2 were used to determine the heat removal for each segment. Each segment was assumed to have no conductance to the segments on either side of it. While the number of segments may eventually become overwhelming from a fabrication and deployment standpoint, the development of variable temperature radiators is a gap that needs to be closed.

C. Cryocoolers

The cryocoolers were modeled as a function of the Carnot Efficiency as shown in Eq 6. The input power for the cryocoolers was then determined based on the relative efficiency related to the Carnot efficiency as shown in Eq 7. The relative efficiency, A in Eq 7, was varied between 15% and 24% for the intermediate temperature to understand the sensitivity of the system to the intermediate temperature cryocooler performance. For the purposes of the study, the 20 K cryocooler was assumed to be 15% of Carnot, through recent testing showed that it may perform as well as 20% of Carnot[12]. The effect of an improved cryocooler efficiency at 20 K would serve to skew the system slightly towards higher intermediate temperatures.

$$\eta_{Carnot} = \frac{T_c}{T_h - T_c}, \tag{6}$$

$$\dot{Q}_{input} = A\eta_{Carnot}\,\dot{Q}_{remove,liquefaction}, \tag{7}$$

V.Results and Sensitivities

For evaluation purposes, let us assume a production rate of 0.3 kg/hr of hydrogen, a production rate of about 20 metric tons of propellant per year at ratios as would be consumed by an oxygen hydrogen rocket engine[5]. At this level, all assumptions are that the analysis scales directly with production rate (so a production rate of double the hydrogen would double the radiator size and system masses). For the base case, we consider the hydrogen flow rate coming in at 300 K (temperatures between the exit temperature of the electrolysis unit and 300 K can easily be handled by a radiator), the vapor being cooled to saturation and liquefied by a 20 K cryocooler. This requires approximately 330 W of heat rejection on the cryocooler. Since it is at 20 K, the required input power is 35 kW and the radiator size to reject 35.3 kW is 85 m^2.

Another point of comparison is a radiator only hydrogen system, cooling down from 300 K to 90 K in a staged approach requires 290 W of heat rejection. Calculating the area required every 5 K, the required radiator area is 14 m^2 (a flux of just over 21 W/m^2). However, 110 W still needs to be rejected (not including the conversion of ortho-hydrogen to para-hydrogen) to cool the gas down to 20 K and account for the phase change. Continuing in the same method, a total of 1300 m^2 of radiator is found to be needed, this is approximately 0.32 acres. Attempting to build a radiator of that size on the lunar surface, while it will eventually need to be done for larger systems, doing this for an initial capability system is a stretch and makes even the single stage 20 K cryocooler look appealing.

At this point, it becomes interesting to investigate two or more stages of cooling as described by the three systems above. The first case evaluated is the radiative precooler (Figure 1). Input power (Figure 4) and radiator area (Figure 5) are shown as a function of radiator exit temperature and at different radiator emissivities. The input power is shown to significantly decrease due to the amount of thermodynamic energy being rejected by the radiator. However, the radiator areas increase significantly. The radiator area's forth order sensitivity to temperature is easily seen as the system gets colder. However, with exit temperatures in the 120 K range, the radiator stays small enough with a still significant reduction in input power to make this system of interest.

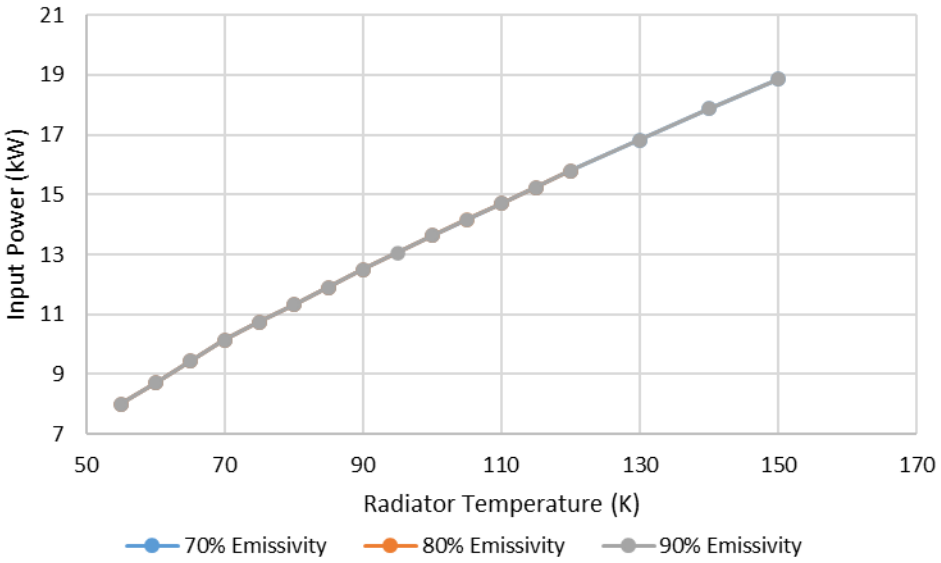

Figure 4: Input power required for radiator precooling only configuration as a function of radiator exit temperature and emissivity.

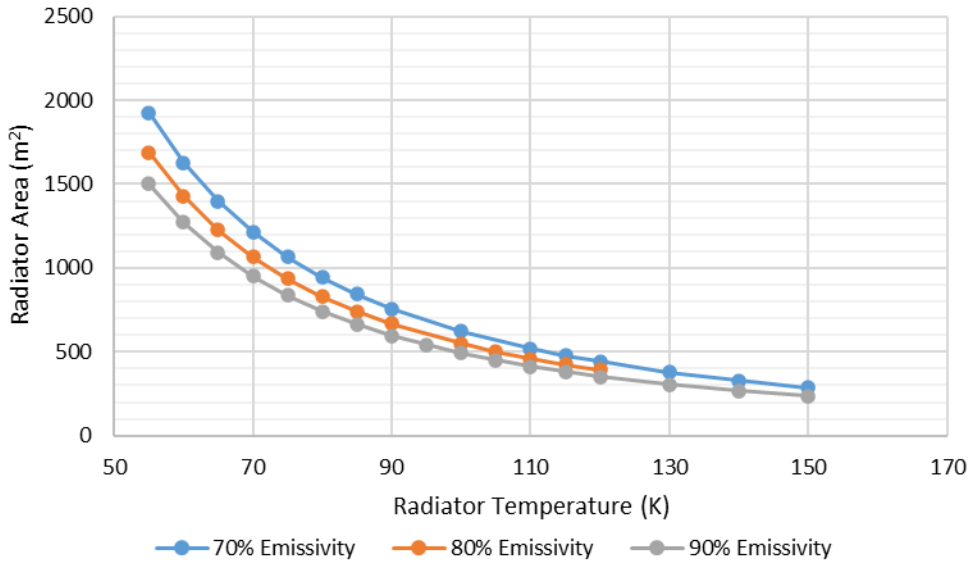

Figure 5: Radiator area required for radiator precooling only configuration as a function of radiator exit temperature and emissivity.

The results for system two, the cryocooler precooling system (Figure 2), showing input power (Figure 6) and radiator size (Figure 7) are shown as a function of intermediate cryocooler temperature. With a 15% of Carnot efficient cryocooler, both input power and radiator mass are at their lowest around 75 K. However, as the efficiency of the cryocooler increases, the intermediate cooling temperature wants to move to the left where it can intercept more sensible energy and convert more hydrogen to para hydrogen at a higher efficiency than the 20 K cryocooler. For the 20% Carnot and 24% Carnot cryocoolers, the intermediate temperatures look to settle out in the 60 to 70 K range. We also see that the both the input power and the radiator area are decreased by a factor of 2-3 from the 20 K cryocooler only case.

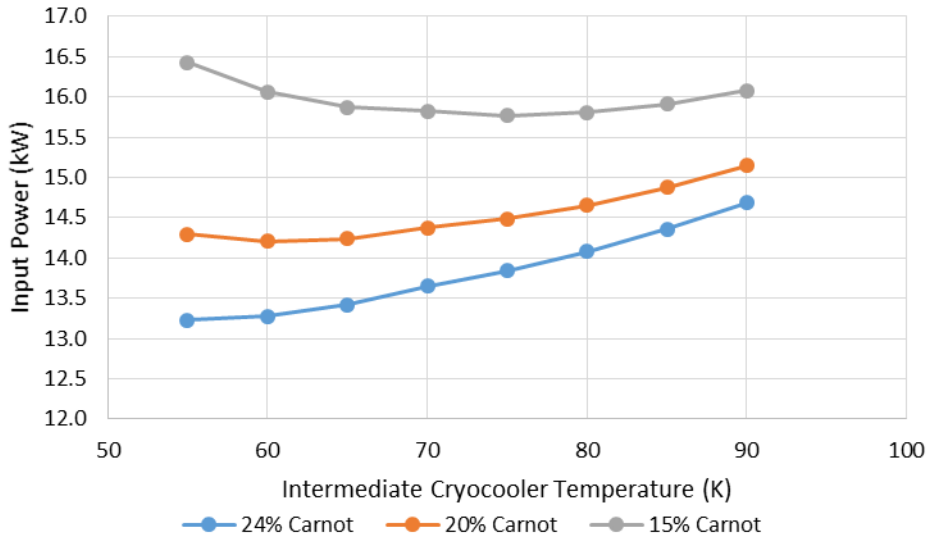

Figure 6: Input power required for a intermediate temperature cryocooler solution as a function of intermediate cryocooler temperature and efficiency.

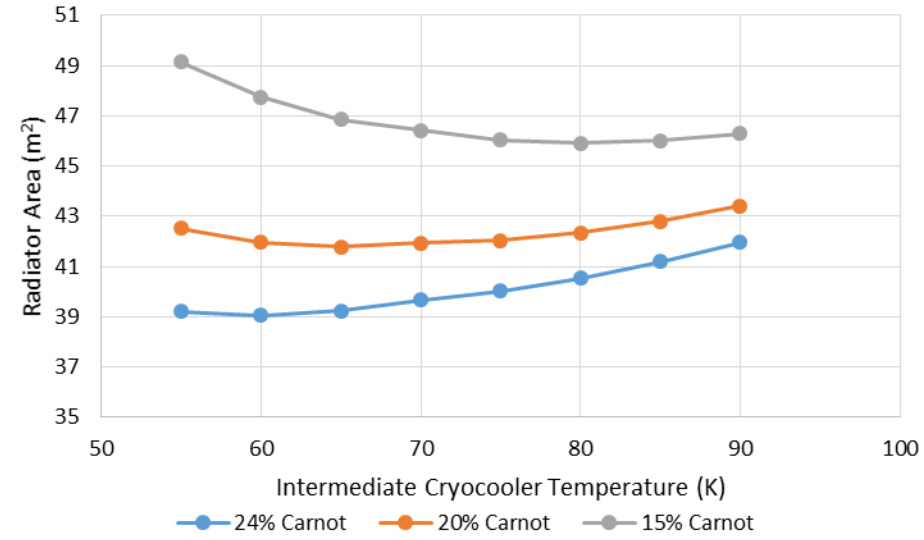

Figure 7: Radiator area required for a intermediate temperature cryocooler solution as a function of intermediate cryocooler temperature and efficiency.

The final configuration of interest is the combination of a pre-cooling radiator and a cryocooler (see Figure 3) as the results from the first two cases show that putting a cryocooler in front of a radiator would not be practical in implementation. In this third scenario, we put the pre-cooling radiator upstream of the first cryocooler. Based on the results seen in the first two analysis, keeping the radiator temperature above 120 K is required, for this investigation, we set it at 150 K to take a bit better advantage of the intermediate temperature cryocooler in combination with it. This precooling radiator is only about 3 m^2 and has some large benefits. Figure 8 shows the updated input power sensitivity trade and Figure 9 shows the updated radiator sensitivity trade. We see that the pre-cooling radiator reduces both the input power and the radiator area by another 20% from option two. With the curves not indicating any level of minimum between the intermediate cryocooler stage temperatures of 50 K and 90 K. This trade could be performed on a single point as a function of pre-cooler temperature as well. Compared to option 2, it is clear that the preferred intermediate cryocooler temperatures are considerably lower with the benefits increasing with lower efficiency cryocooler and lower intermediate temperature solutions.

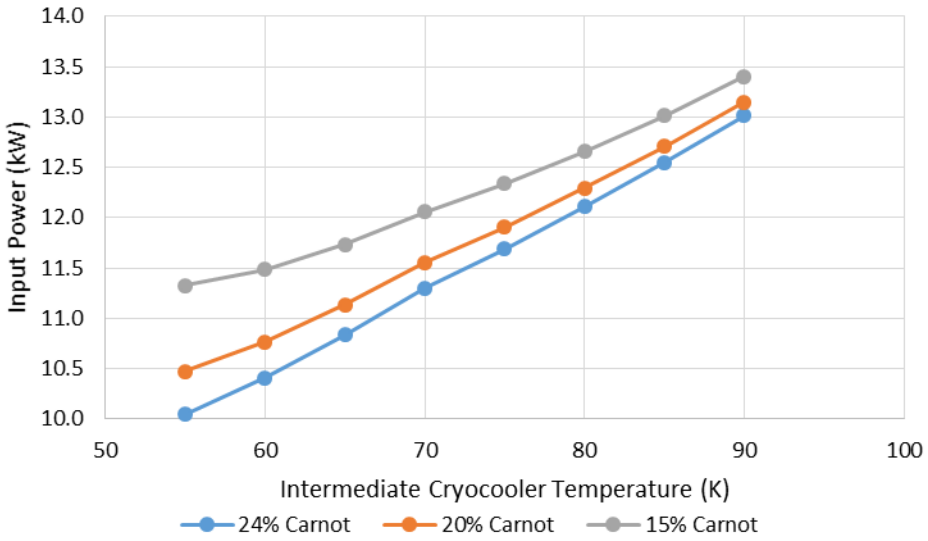

Figure 8: Input power required for a intermediate temperature cryocooler with 150 K pre-cooling radiator solution as a function of intermediate cryocooler temperature and efficiency.

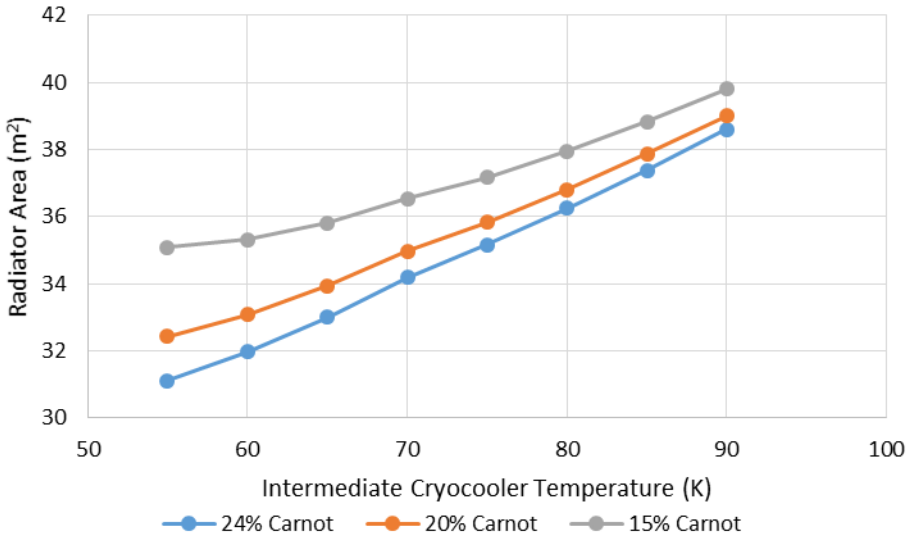

Figure 9: Radiator area required for a intermediate temperature cryocooler solution with 150 K precooling radiator as a function of intermediate cryocooler temperature and efficiency.

The cryocooler heat removal requirements as a function of intermediate cryocooler temperature are shown for all the cases in Figure 10. The 20 K cryocooler lift requirements are the same for all three cases as it is not impacted by what provides the precooling and varies between 70 W and 100 W. The intermediate cryocooler is not needed in the radiator only precooling case, varies between 260 W and 230 W in the cryocooler precooling only case, and varies between 50 W and 100 W (a reduction of 2.5 – 4 times) with a 150 K radiator in front of it. To understand just how dominant the 20 K cryocooler power is, we can see that while the intermediate temperature cryocooler requirements drop by such a large amount, the system level power requirements only drop around 20%.

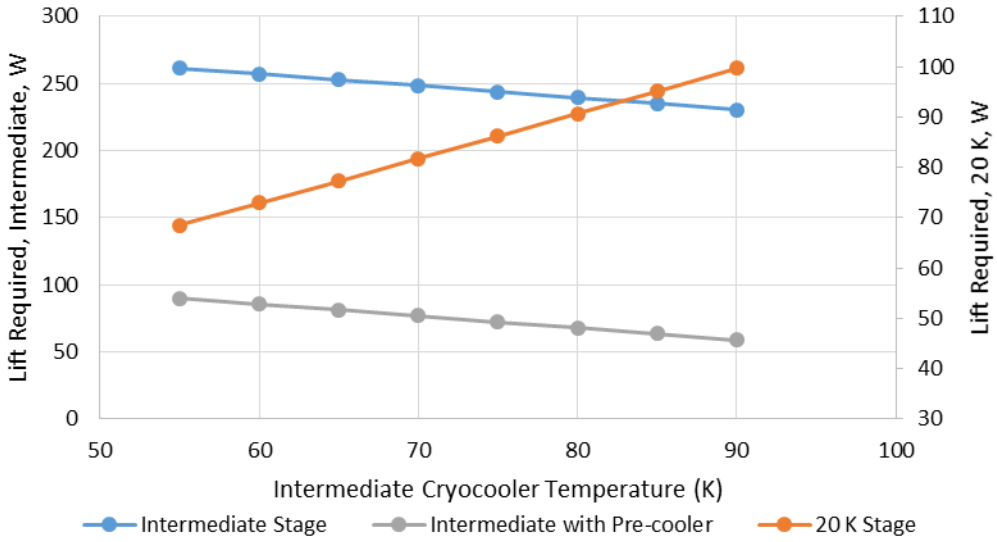

Figure 10: Cryocooler lift required at both 20 K and an intermediate temperature as a function of the intermediate temperature for all three cases with precooling.

Further analysis was performed adjusting several parameters individually. First, during Martian liquefaction trades conducted by Oleson et al[13], it was determined that Martian radiators would have a hard time getting below 250 K. Thus, the radiator and cryocooler precooling case was run again, but with the precooling radiator at 250 K compared

to 150 K. The results from the run are shown in Figure 11. The overall increase in input power ranges between 8% to 30% compared to the 150 K radiator and intermediate cryocooler precooling, with the increase in input power increasing with both decreasing intermediate cryocooler temperature and decreasing intermediate cryocooler efficiency. Power minimums at temperatures above 55 K started to appear at the lower efficient intermediate cryocoolers. While this change does not affect the 20 K cryocooler heat removal requirements, it increases the intermediate cryocooler heat removal requirements by a factor of 2.2 to 2.9, increasing with increasing intermediate cryocooler temperature (as seen in Figure 12).

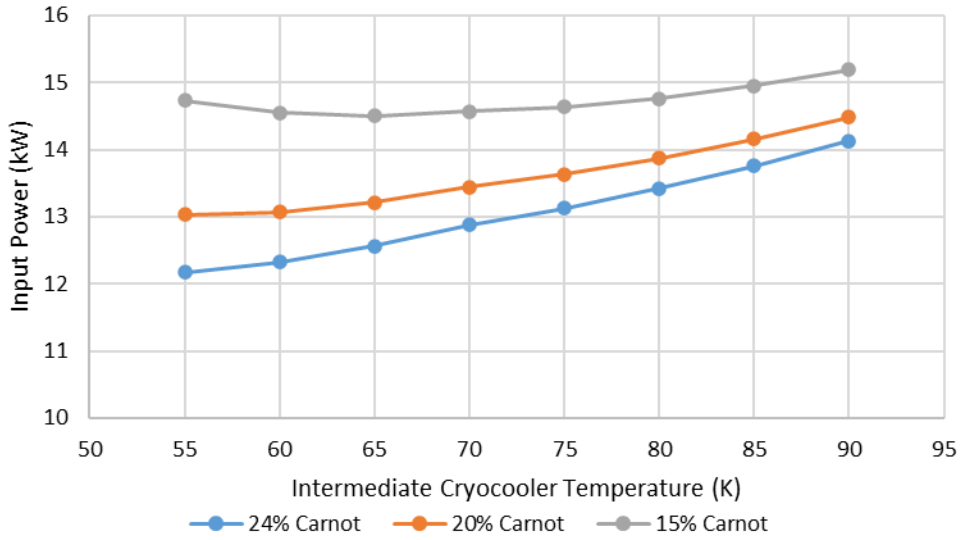

Figure 11: Input power required for a intermediate temperature cryocooler with 250 K pre-cooling radiator solution as a function of intermediate cryocooler temperature and efficiency.

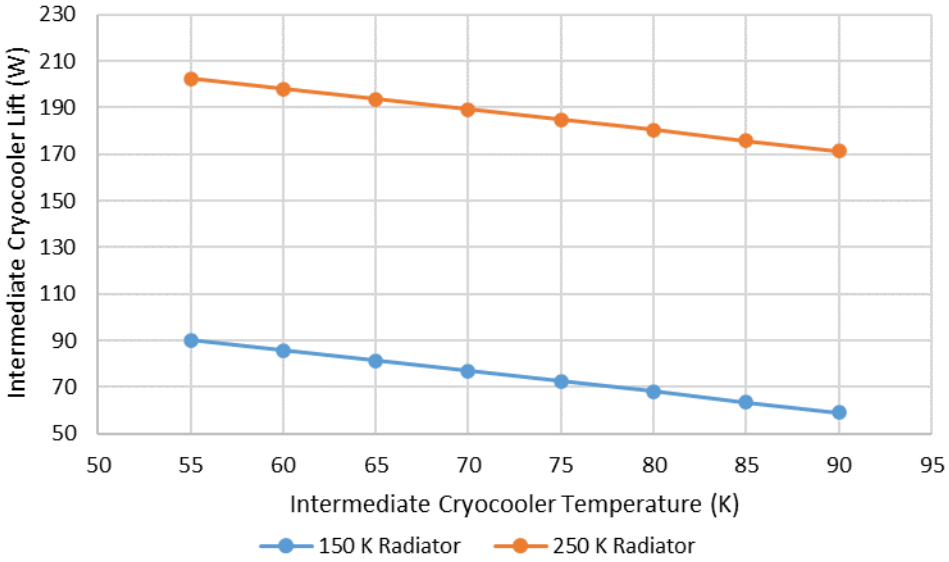

Figure 12: Heat removal powers for the intermediate cryocooler as a function of temperature for 150 K and 250 K radiator precoolers.

The trades above focus on the efficiency of the intermediate temperature cryocooler, however the efficiency of the 20 K cryocooler also can affect the trade results. Adjusting the 20 K cryocooler performance from 15% Carnot to 20% Carnot, the combined radiator and intermediate temperature precooling condition was rerun. The results are

shown in Figure 13. The total input power decreased by 18 – 25% with increasing input power benefit at higher intermediate cryocooler temperature as would be expected due to the added power at 20 K higher intermediate cryocooler temperatures require. This would not change the cryocooler lift requirements, only the power requirements.

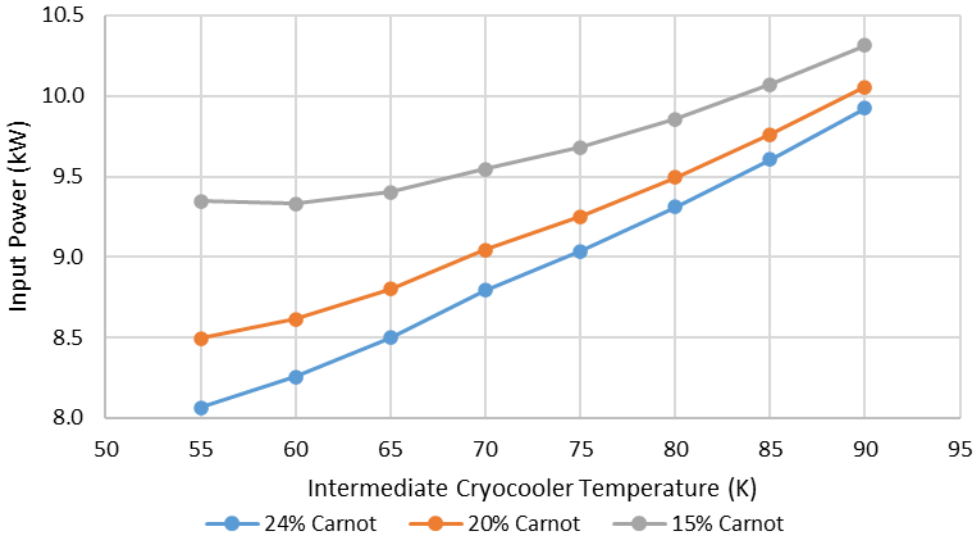

Figure 13: Input power required for an intermediate temperature cryocooler with 150 K pre-cooling radiator solution as a function of intermediate cryocooler temperature and efficiency. 20 K cryocooler efficiency was improved to 20% of Carnot.

VI. Mass Impacts

By assigning areal densities for radiator area and input power mass, we can determine the change in mass. The cryocooler mass will be fairly insignificant in this trade as it is much smaller than the input power mass and radiator mass. Based off of analysis of a Fission Surface Power system[14-16] developed by Lee Mason[17], the power system for a cryocooler, including the power management and distribution (PMAD) system, at 90% efficiency and 100 W/kg, is approximately 178 kg/kW input power required at the cryocooler (the 10 – 35 kW input power required is within scope of multiple Fission Surface Power systems analysis and studies). Similarly, analysis can be done for a double sided deployable radiator for the lunar surface are estimated at 3.9 kg/m^2 of radiator area required[18]. The base case for 35.3 kW input power and 85 m^2 of radiator is 6612 kg. The mass results for the radiator precooling only system are shown in Figure 14 and are very high (much higher than the base 20 K cryocooler only case) due to the high radiator areas required for precooling, especially approaching 55 K. However, as the radiator temperature approaches 120 K, the radiators shrink enough to make the mass an improvement on the baseline. In both cases that are run to 150 K, minimums are seen in the mass curves below 150 K. Figure 15 shows the mass for the intermediate cryocooler precooling only case with minimum masses in similar locations as the minimum power as the mass is driven by the input power, not the radiator. The mass here is dropped by at least 50% compared to the base mass. Figure 16 shows the mass with at 150 K radiative precooler and intermediate cryocooler. The mass with the additional radiator precooling at 150 K is approximately 400 – 500 kg less than the equivalent mass with cryocooler precooling only.

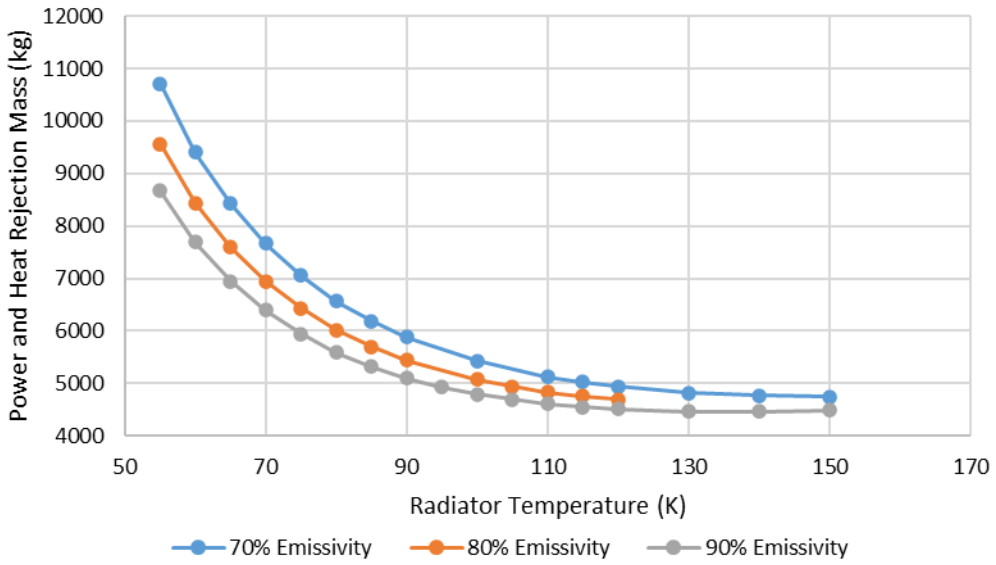

Figure 14: Mass of the power and heat rejection system for the radiator precooling only liquefaction system.

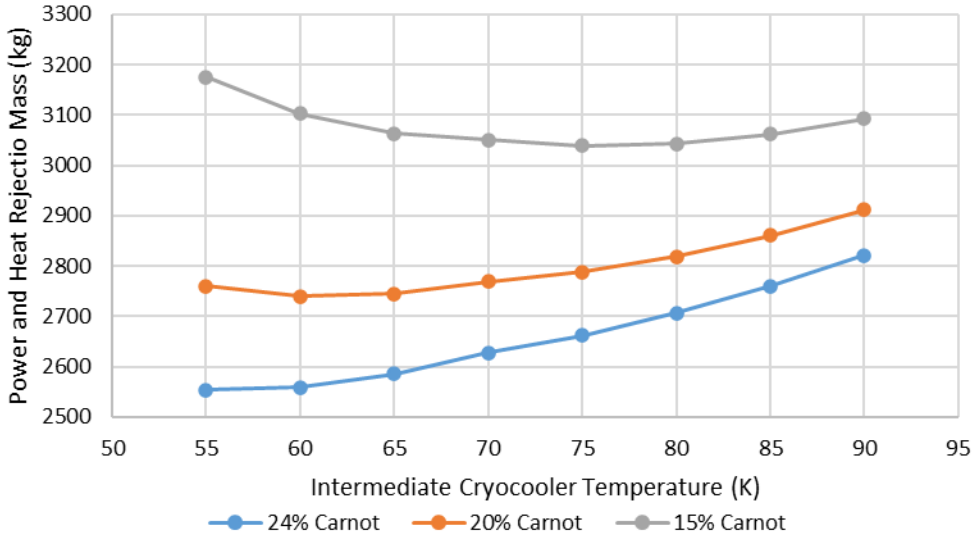

Figure 15: Mass of the power and heat rejection system for the intermediate cryocooler only precooling liquefaction system.

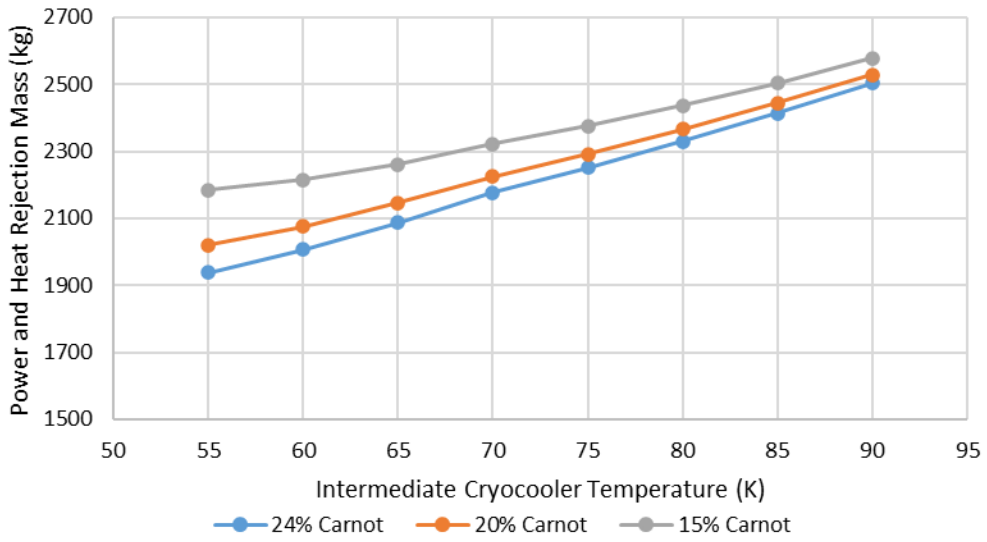

Figure 16: Power and heat rejection system mass required for a intermediate temperature cryocooler solution with 150 K precooling radiator as a function of intermediate cryocooler temperature and efficiency.

VII. Conclusion

It has been shown that the amount of resources (especially power) required for the liquefaction of hydrogen and oxygen in PSRs cannot be assumed to be zero. However, radiators precooling the gas streams to some temperature below 300 K is preferential, but below approximately 120 K, cryocoolers should be used. Both pre-cooler radiators and 70 – 90 K class flight-rated cryocoolers can be used to significantly reduce the input power requirements and radiator area over just 20 K class flight-rated cryocoolers. The benefits of the precoolers can also be coupled with oxygen liquefaction to take advantage of the 90 K class flight-rated cryocoolers that would be required for that system. The trade between input power (and cryocooler mass) and radiator area (including heat exchange between the gas and the radiator) should be explored further as the basis for the resources required to liquefy hydrogen on the Moon either in the permanently shadowed regions or with appropriate adjustments for other regions.

From a technology development standpoint, current activities are on-going for 150 W at 90 K cryocoolers and 20 W at 20 K cryocoolers[12]. One to two of the currently developed 90 K cryocoolers appear to be enough for the 0.3 kg/hr hydrogen liquefaction case in any scenario. However, the 20 K side may need up to five 20 W cryocoolers. This is notionally acceptable for initial surface activities, but as hydrogen demand grows, increased heat removal at 20 K should be investigated. Finally, the high temperature gradient radiators are significantly different than current radiator developments. While the fundamental physics aren't changing, the challenge will be in the thermal isolation (both conductively and radiatively) between the radiator sections while splitting them in a reasonable manner. It is highly probabe that, especially on the warm end of the radiator, 5 K splits are not realistic. While this would increase the radiator sizes from the analyzed numbers, the impact should not be large (seeing that the larger impact will be in the high heat flux area), and the general trends shown should still be correct. Development of these type of radiators should be considered to reduce the system level power required.

Acknowledgments

This work was funded by the NASA Space Technology Mission Directorate's Technology Demonstration Missions Program under the Cryogenic Fluid Management Portfolio Project and by the Exploration Systems Development Mission Directorate under the Advanced Exploration Systems Program's Cryogenic Fluid In-situ Liquefaction for Landers (CryoFILL) project. The initial excel model was developed by Chris Dardano as a part of his internship activities.

References

[1] Mitchell, J., S. Lawrence, M. Robinson, E. Speyerer, B. Denevi (2017), Using complementary remote sensing techniques to assess the presence of volatiles at the lunar north pole, *Planetary and Space Science*, doi: 10.1016/j.pss.2017.07.015.

[2] https://www.nasa.gov/topics/solarsystem/features/divinerb20090917.html

[3] Metzger, P.T., "Space development and Space Science Together, an Historic Opportunity", Space Policy, 37, 77-91, 2016.

[4] Kornuta, D., et. al., "Commercial Lunar Propellant Architecture", https://www.ulalaunch.com/docs/default-source/commercial-space/commercial-lunar-propellant-architecture.pdf?sfvrsn=649113d4_4

[5] Sanders, G. In Situ Resource Utilization (ISRU) - Surface Excavation and Construction. Presented to the NASA Advisory Council: Technology, Innovation, and Engineering Committee, Jan 21, 2021.

[6] https://www.nasa.gov/viper/overview

[7] Johnson, W.L., Grotenrath, R.J., Balasubramaniam, R., Chan, H.M., Smith, J.W., and Giddents, P.A., "Cryogenic Fluid In-Situ Liquefaction for Landers: Prototype Demonstration", presented at ASCEND 2023, Oct 23-25, 2023.

[8] Bliesner, R.M., Leachman, J.W., and Adam, P.M., Parahydrogen-Orthohydrogen Conversion for Enhanced Vapor-Cooled Shielding of Liquid Oxygen Tanks, Journal of Thermophysics and Heat Transfer, Vol. No., 2014.

[9] Nugent, B. T., Johnson, W. L., Guzik, M. C., & Stephens, J. R. Space Exploration Applications for Development of High Capacity Cryocoolers. Cryocoolers 21, edited by R.G. Ross, Jr, J.R. Raab, and S.D. Miller. Boulder, CO, 2021

[10] Lemmon, E.; Huber, M.; and McLinden, M.: NIST Standard Reference Database 23: Reference Fluid Thermodynamic and Transport Properties-REFPROP, Version 9.1, 2013. https://www.nist.gov/publications/niststandard-reference-database-23-reference-fluidthermodynamic-and-transport Accessed Dec. 9, 2020.

[11] Flynn, T. M., "Cryogenic Engineering" New York: Marcel Dekker., 1997.

[12] Nugent, B.T., Grotenrath, R.J., and Johnson, W.L., "20 Watt 20 Kelvin Reverse Turbo-Brayton Cycle Cryocooler Testing and Applications", Cryocoolers 22, ed. Ross Jr, R.G., Raab, J., and Miller, S.D., ICC Press, Boulder CO, 2022, pg 327-334.

[13] Oleson, S.R., Kleinhenz, J.E., and Johnson, W.L., "Kiloton Class ISRU Systems for LOX/LCH4 Propellant Production on the Mars Surface", accepted for presentation at the AIAA SciTech 2024 Forum, Jan 8-12, 2024.

[14] Mason, L.S., "A Comparison of Fission Power System Options for Lunar and Mars Surface Applications", NASA TM-2006-214120, 2006.

[15] Mason, L.S. and Poston, D.I., "A Summary of NASA Architecture Studies Utilizing Fission Surface Power Technology", NASA TM-2011-216819, 2011.

[16] Mason, L.S., Gibson, M., and Poston, D., "Kilowatt-Class Fission Power Systems for Science and Human Precursor Missions", NASA TM-2013-216541, 2013.

[17] Personal communications with Lee Mason

[18] Colozza, A.J., "Small Lunar Base Camp and In-Situ Resource Utilization Oxygen Production Facility Power System Comparison.", NASA TM-20200001622, 2020.